

Sl. No.	<p style="text-align: center;">IIT Ropar List of Recent Publications with Abstract Coverage: October, 2021</p>
1.	<p>A Framework for Partitioning Support Vector Machine Models on Edge Architectures M Sahi, M Al Maruf, A Azim, N Auluck - IEEE International Conference on Smart Computing, 2021</p> <p>Abstract: Current IoT applications generate huge volumes of complex data that requires agile analysis in order to obtain deep insights, often by applying Machine Learning (ML) techniques. Support vector machine (SVM) is one such ML technique that has been used in object detection, image classification, text categorization and Pattern Recognition. However, training even a simple SVM model on big data takes a significant amount of computational time. Due to this, the model is unable to react and adapt in real-time. There is an urgent need to speedup the training process. Since organizations typically use the cloud for this data processing, accelerating the training process has the advantage of bringing down costs. In this paper, we propose a model partitioning approach that partitions the tasks of Stochastic Gradient Descent based Support Vector Machines (SGD-SVM) on various edge devices for concurrent computation, thus reducing the training time significantly. The proposed partitioning mechanism not only brings down the training time but also maintains the approximate accuracy over the centralized cloud approach. With a goal of developing a smart objection detection system, we conduct experiments to evaluate the performance of the proposed method using SGD-SVM on an edge based architecture. The results illustrate that the proposed approach significantly reduces the training time by 47%, while decreasing the accuracy by 2%, and offering an optimal number of partitions.</p>
2.	<p>A vascularized bone-on-a-chip model development via exploring mechanical stimulation for evaluation of fracture healing therapeutics B Das, SV Seesala, P Pal, T Roy, PG Roy, S Dhara - In vitro models, 2021</p> <p>Abstract: Bone is the major connective tissue maintaining the structural integrity of the human body. However, fracture and many skeletal degenerative diseases can compromise this function. Thus, therapeutics related to bone degeneration are of significant research interest and require good in vitro models for such therapeutic evaluation. Bone is a highly vascularized tissue and incorporation of this feature is significantly important for mimicking the osteogenic microenvironment. In the current study, we developed a vascularized flat bone model via simultaneous mechanical actuation of mechanical strain and fluid shear. The mechanical strain was achieved by static magnetic field actuation of a magnetic nanocomposite scaffold. The fluid shear was generated by developing a micropattern on the magnetic nanocomposite via replica molding and laser-based microfabrication. From the live cell imaging window of the microdevice, both bone and vasculature like cellular morphology was observed. The SEM study showed thick ECM deposition in the dynamic culture. In the PCR study, both osteogenic (Col-1, osteocalcin) and angiogenic phenotypes (PECAM) were observed in the dynamic culture scaffolds while chondrogenic marker (Col-2) was downregulated.</p>
3.	<p>An Integrated Driving/Charging 4-Phase Switched Reluctance Motor Drive with Reduced Current Sensors for Electric Vehicle Application V Shah, S Payami - IEEE Journal of Emerging and Selected Topics in Power Electronics, 2021</p> <p>Abstract: The paper proposes an integrated power converter (IPC) with driving/charging capabilities for 4-phase switched reluctance motor (SRM) drive based electric vehicle (EV) application. With the proposed IPC, only two current sensors are employed for measuring phase currents under all operating conditions. The proposed IPC integrates three circuits. Firstly, during the SRM driving mode, the proposed IPC is utilized as an improved miller converter. Secondly, during battery charging mode, the proposed IPC is utilized as an on-board battery charger which is based on a bridgeless boost power factor correction circuit (PFCC) that incorporates two DC-DC</p>

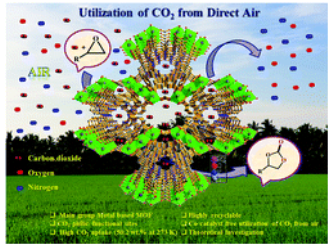
	<p>boost converters. The on-board battery charger is realized by utilizing the existing power electronic switches in the proposed IPC and all the phase windings as charging inductors. Third, a front-end bidirectional DC-DC converter for maintaining voltage and current balance between IPC DC-bus and battery. During driving mode, the front-end converter boosts the battery voltage to the IPC DC bus voltage. And during regeneration/braking, the stored magnetic energy is used to charge the battery in constant-current (CC) mode via the front-end converter. During battery charging via AC grid, the bridgeless boost PFCC and the front-end converter operating in buck mode charges the battery in CC/ constant-voltage (CV) modes without stepping down the AC grid voltage. The claims of the proposed IPC are validated through simulation and experimental verifications.</p>
4.	<p>Analytical Study of Frequency Modulated Thermography for Defect Estimation in Carbon Fibre Reinforced Polymer A Rani, V Arora, KR Sekhar, R Mulaveesala - International Conference on Signal Processing and Integrated Networks, 2021</p> <p>Abstract: Frequency modulated thermography (FMT) is an efficient thermographic technique for quantitative analysis of defects in any material. The paper presents analytical solution of heat transfer in a finite thickness sample with flat bottom hole defects located at different lateral dimensions. The carbon fibre reinforced polymer (CFRP) sample is subjected to frequency modulated thermal excitation and temperature variations are evaluated for defect detection analysis. The computed analytical solutions for different defect depths have been shown to agree with corresponding simulation results for CFRP sample. The present work highlights defect detection capability of FMT technique using matched filter approach.</p>
5.	<p>Arylcyclopropane yet in its infancy: the challenges and recent advances in its functionalization IM Taily, D Saha, P Banerjee - Organic & Biomolecular Chemistry, 2021</p> <p>Abstract: Electronically unbiased arylcyclopropane functionalization has always been a challenge to organic chemists, and the emergence of donor–acceptor cyclopropanes (DACs) has not only vehemently overshadowed them but still dominates the cyclopropane chemistry. Unlike DACs, the absence of pre-installed functional groups makes it harder for them to activate and participate in a reaction. The field has witnessed considerably slow progress since its inception due to the inherent challenges. There are only a few strategies available to open arylcyclopropanes. Therefore, this work is still in its infancy stage in spite of these materials being one of the earliest known type of cyclopropanes. This review manifests the history, endeavors, and achievements alongside the associated challenges, opportunities, and the need for concerted efforts to accomplish the long-awaited golden age of arylcyclopropanes.</p>
6.	<p>Boron-Catalyzed Hydroarylation of 1, 3-Dienes with Arylamines G Kumar, ZW Qu, S Grimme, I Chatterjee - Organic Letters, 2021</p> <p>Abstract: Catalytic hydroarylation reactions of conjugated dienes are achieved using tris(pentafluorophenyl)borane as a Lewis acid catalyst under mild reaction conditions. This new protocol shows a broad substrate scope for the highly regioselective functionalization of sterically hindered aniline derivatives. Experimental and extensive density functional theory mechanistic studies show that the complex of residual water and $B(C_6F_5)_3$ plays a crucial role in the aryl-assisted protonation of conjugated dienes, forming allyl cation intermediates that induce the facile electrophilic aromatic substitution of aniline substrates.</p>
7.	<p>Characterization and Slurry Erosion Mechanisms of Nickel-Based Cermet Coatings on Monel K-500 NK Singh, A Kumar, ASM Ang, DK Mahajan, H Singh - Journal of Thermal Spray Technology, 2021</p> <p>Abstract: Monel K-500 is a nickel-based alloy broadly used in several industries such as power generation, aerospace, marine and chemical processing for manufacturing several critical</p>

	<p>components. During hydraulic applications, the alloy is subjected to different degradation phenomena such as cavitation erosion, slurry erosion and corrosion. The current study assesses the potential of using two HVOF-sprayed nickel-based cermet coatings: WC-10Ni-5Cr and WC-18Hastelloy C to control the slurry erosion of Monel K-500. The coatings were subjected to slurry erosion tests for 90 min at normal (90°) and oblique (30°) impingement angles. It was observed that these coatings significantly reduced the erosive wear in Monel alloy. WC-10Ni-5Cr coating, having relatively better microhardness and fracture toughness has shown minimum erosion losses. At normal impact, WC-10Ni-5Cr coating and WC-18Hastelloy C coating reduced the erosion rate of Monel by 2.3 and 1.6 times, respectively. At oblique impact, WC-10Ni-5Cr coating and WC-18Hastelloy C coating reduced the erosion rate of Monel by 4.75 and 2.4 times, respectively. In-depth study of the erosion mechanism for the investigated materials was conducted using scanning electron microscopy. Ploughing and micro-cutting were the primary erosion mechanisms in Monel alloy, whereas coating spallation and crater formation were the primary erosion mechanisms in the coatings.</p>
8.	<p>Competing thermal and solutal advection decelerates droplet evaporation on heated surfaces A Kaushal, V Jaiswal, V Mehandia, P Dhar - <i>European Journal of Mechanics-B/Fluids</i>, 2021</p> <p>Abstract: We report the complex evaporation kinetics of saline sessile droplets on surfaces with elevated temperatures. Our previous studies show that on non-heated substrates, saline sessile droplets evaporate faster compared to the water counterparts. In the present study, we discover that on heated surfaces, the saline droplets evaporate slower than the water counterpart, thereby posing a counter-intuitive phenomenon. The reduction in the evaporation rates is directly dependent on the salt concentration and the surface wettability. Natural convection around the droplet and thermal modulation of surface tension is found to be inadequate to explain the mechanisms. Flow visualisations using particle image velocimetry (PIV) reveal that the morphed advection within the saline droplets is a probable reason behind the arrested evaporation. Infrared thermography is employed to map the thermal state of the droplets. A thermo-solutal Marangoni based scaling analysis is put forward and the major governing non-dimensional numbers have been accounted for in the analysis. It is observed that the Marangoni flow and internal advection borne of thermal and solutal gradients are competitive, thereby leading to the overall decay of internal circulation velocity compared to the equivalent pure water case, which reduces the evaporation rates. The theoretically proposed advection velocities conform to the experimental results. This study sheds rich insight on a novel species transport behaviour in saline droplets.</p>
9.	<p>Designing Bounded Min-Knapsack Bandits Algorithm for Sustainable Demand Response A Singh, PM Reddy, S Jain, S Gujar - <i>Pacific Rim International Conference on Artificial Intelligence: Part of the Lecture Notes in Computer Science book series</i>, 2021</p> <p>Abstract: Recent trends focus on incentivizing consumers to reduce their demand consumption during peak hours for sustainable demand response. To minimize the loss, the distributor companies should target the right set of consumers and demand the right amount of electricity reductions. Almost all the existing algorithms focus on demanding single unit reductions from the selected consumers and thus have limited practical applicability. Even for single unit reductions, none of the work provides a polynomial time constant approximation factor algorithm to minimize the loss to the distributor company. This paper proposes a novel bounded integer min-knapsack algorithm (MinKPDR) and shows that the algorithm, while allowing for multiple unit reduction, also optimizes the loss to the distributor company within a factor of two (multiplicative) and a problem dependant additive constant. The loss is a function of the cost of buying the electricity from the market, costs incurred by the consumers, and compliance probabilities of the consumers. When the compliance probabilities of the consumers are not known, the problem can be formulated as a combinatorial multi-armed bandit (CMAB) problem. Existing CMAB algorithms fail to work in this setting due to the non-monotonicity of a reward function and time varying optimal sets. We propose a novel algorithm (Twin-MinKPDR-CB) to learn these compliance probabilities</p>

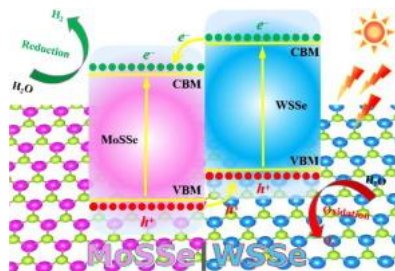
	efficiently. Twin-MinKPDR-CB works for non-monotone reward functions, bounded min-knapsack constraints, and time-varying optimal sets. We theoretically show that Twin-MinKPDR-CB achieves sub-linear regret of $O(\log T)$ with T being the number of rounds for which demand response is run.
10.	<p>Detection of inaccessible head and neck lesions using human saliva and fluorescence spectroscopy P Kumar - Lasers in Medical Science, 2021</p> <p>Abstract: Head and neck cancer detection using fluorescence spectroscopy from human saliva is reported here. This study has been conducted on squamous cell carcinoma (SCC), and dysplastic (precancer) and control (normal) groups using an in-house developed compact set-up. Fluorescence set-up consists of a 375-nm laser diode and optical components. Spectral bands of flavin adenine dinucleotide (FAD), porphyrins, and Raman are observed in the spectral range of 400 to 800 nm. Presence of FAD and porphyrin bands in human saliva is confirmed by the liquid phantoms of FAD and porphyrin. Significant differences in fluorescence intensities among all the three groups are observed. Three spectral ranges from 455 to 600, 605 to 770, and 400 to 800 nm are selected for each group and area values under each spectral range are computed. To differentiate among the groups, receiver operating characteristic (ROC) analysis is employed on the area values. ROC differentiates among the groups with accuracies of 98%, 92.85%, and 81.13% respectively in the spectral ranges of 400 to 800 nm. However, in other two spectral ranges (455 to 600 and 605 to 770 nm), low accuracy values are found. Obtained accuracy values indicate that selection of human saliva for head and neck cancer detection may be a good alternative.</p>
11.	<p>Dynamics between trade openness, FDI and economic growth: evidence from an emerging economy B Rakshit - Journal of International Trade Law and Policy, 2021</p> <p>Abstract: Purpose This paper aims to examine the dynamics between trade openness, foreign direct investment (FDI) and economic growth in India over the period 1979 to 2017. This study further considers the role of pre and post-economic reforms in the analysis of these dynamics.</p> <p>Design/methodology/approach The authors apply the autoregressive distributed lag model to investigate the possible long-run associations among the variables. Zivot-Andrew unit root test was applied to detect the structural breaks present in the data series. Toda-Yamamoto causality approach has been applied to examine the direction of causality among the variables.</p> <p>Findings Findings show that trade openness exerts a negative impact on economic growth in the long-run. Although FDI inflow promotes economic growth in the long-run, FDI inflow does not seem to affect growth in the short-run. As far as causality analysis is concerned, findings confirm a unidirectional causality is flowing from FDI inflow and labour force to per capita gross domestic product growth in India.</p> <p>Practical implications The negative impact of trade openness on growth suggests that policymakers should implement more export-oriented policies to boost economic growth in the long-run. The ratio of exports to the total volume of trade has not increased satisfactorily over the years. Additionally, appropriate policies should aim at extracting the benefits of FDI inflow in the long-run.</p> <p>Originality/value Although several theoretical and empirical literature has investigated the nexus between FDI (or trade) and growth, this study, as a fresh attempt, investigates the long-run dynamics between trade</p>

	openness, FDI, capital formation, labour force and economic growth in India.
12.	<p>Dynamics of capital account and current account in India: Evidence from threshold cointegration with asymmetric error correction L Mallick, SR Behera, RVR Murthy - <i>Applied Economics Letters</i>, 2021</p> <p>Abstract: This study investigates the nexus between India's current and capital accounts using threshold cointegration and asymmetric error-correction approaches. The results validate the threshold cointegration between the current account (CA) and India's capital account (KA). The asymmetric error correction-based results support the unidirectional Granger causality from KA to CA. Further, results reveal that KA's cumulative sum of positive and negative deviation substantially impacts the CA. Finally, results of equilibrium adjustment path asymmetric effect from CA to KA suggest that KA reverts to equilibrium in the short run when CA decreases.</p>
13.	<p>Effect of organic matrix alteration on strain rate dependent mechanical behaviour of cortical bone P Uniyal, P Sihota, N Kumar - <i>Journal of the Mechanical Behavior of Biomedical Materials</i>, 2021</p> <p>Abstract: The organic matrix phase of bone plays important role in its mechanical performance, especially in the post-yield regime. Also, the organic phase influences loading rate-dependent behaviour of bone which is relevant during the high-speed loading events. Many diseases, as well as aging, affect the matrix phase of bone which causes compromised mechanical properties. Improved understanding of alterations in the organic matrix phase on mechanical response of bone will be helpful in the mitigation of fractures associated with inferior matrix quality. In the present work, effect of alteration in organic matrix of cortical bone on its strain-rate dependent behaviour was investigated. To produce different amounts of collagen denaturation, bovine cortical bones were heated at the temperature of 180 °C and 240 °C. Further, compression testing was performed at quasi-static strain rates of 10–4 s⁻¹ to 10–2 s⁻¹ using a conventional testing machine whereas a modified Split Hopkinson Pressure Bar (SHPB) was used for high strain rate (~103) testing. Thermal treatment-induced changes in the mineral and organic phases of bone were assessed using X-ray diffraction (XRD) and Fourier-transform infrared-attenuated total reflection (FTIR-ATR) techniques respectively. Compression test results show that thermal treatment of bone up to 180 °C did not affect mechanical properties significantly whereas treating at 240 °C significantly reduced elastic modulus, failure stress and failure strain. Also, thermal denaturation of collagen reduced the strain rate sensitivity of cortical bone at high strain rates. Similar to the compression test observations, nanoindentation results show a significant reduction in elastic modulus and hardness of denatured samples. Further, FTIR results revealed that with the heat treatment of bone, collagen structure undergoes conformational changes at the molecular level. The initial helix structure breakdowns into unordered/random coil structures which subsequently reduced the mechanical competence of bone. The present study provides insight into the effect of organic matrix modification on mechanical behaviour of cortical bone which could be helpful in understanding bone disorders associated with organic matrix phase and development of therapeutic interventions.</p>
14.	<p>Effect of Revised Seismic Design Provisions on Seismic Performance of RC Frame Buildings with and Without Infills PL Kurmi, P Halder - <i>Emerging Technologies and Applications for Green Infrastructure: Part of the Lecture Notes in Civil Engineering book series</i>, 2021</p> <p>Abstract: Indian Standard for seismic design of Reinforced Concrete (RC) frame buildings with Un-Reinforced Masonry (URM) Infills have undergone significant revisions in 2016 compared to its older version in 2002 and 1993, respectively. Two of the major revisions of BIS 13920-2016 are the inclusion of capacity design criteria to ensure strong-column weak-beam and selection of column dimension based on largest longitudinal beam rebar. The revised seismic design standard also recommends modeling guidelines for Un-Reinforced Masonry (URM) infill using the equivalent diagonal strut to take into account the complex infill-frame interaction. Under lateral loading, infills contribution to global strength and stiffness is often ignored for being treated as</p>

	<p>non-structural elements in general design practice. The present study attempts to evaluate the comparative seismic response of Special Moment Resisting Frame (SMRF) RC buildings with and without infills, designed with revised and older versions of Indian seismic standards. Capacity curves have been developed through nonlinear static pushover analysis. It has been observed that revised code provisions improve the structural performance in terms of stiffness, strength, inelastic displacement capacity, and eventually results in the desired ductile failure mechanism of the RC frames. However, considering the effect of infills as per the revised Indian standard has led to reduced inter-storey drift and ultimate inelastic deformation compared to the bare frame and the general design practice. It has been observed that the infill-frame interaction plays a key role in the overall performance as well as govern the failure mechanism of the structure as a whole.</p>
15.	<p>Effect of Structural Wall Plan Density on Performance of RC Shear Wall Buildings Designed as Per Indian Standards KKK Reddy, P Halder - Emerging Technologies and Applications for Green Infrastructure: Part of the Lecture Notes in Civil Engineering book series, 2021</p> <p>Abstract: Reinforced Concrete (RC) shear wall buildings are the most common construction practice in moderate to high seismic zones. Shear walls provide high strength, stiffness to the building system. However, the performance of RC shear wall buildings depends on various parameters like the location of shear walls, the aspect ratio of the shear wall, and the structural wall plan density. The revised Indian standards for earthquake-resistant design of structures states that RC structural wall plan density shall be at least 2% for buildings with open storeys, and for regular buildings it can be at least 2% along each principal direction. This manuscript aims to check the efficacy of the minimum structural plan density recommended in the revised Indian standard by evaluating the impact of varying structural wall density on the seismic performance of high-rise regular RC shear wall buildings located in the high seismic zone. The seismic performance of shear wall buildings with varying structural wall density is evaluated in terms of peak displacements, peak accelerations, and maximum inter-story drift by performing the time history analysis with different ground motion records. The effect of structural wall plan density on the dynamic properties of the buildings is also studied.</p>
16.	<p>Effect of Substrate Inclination on Post-impact Dynamics of Droplets N Sahoo, D Samanta, P Dhar - Advances in Thermofluids and Renewable Energy, 2022</p> <p>Abstract: Understanding of impact dynamics of droplets on oblique plane is relevant for applications like pesticides spraying and internal combustion engines. Experiments were performed using three test fluids to investigate the effect of viscosity and surface tension properties on the elongation factor of droplets impacting on oblique planes. The temporal variation of elongation factor primarily depends upon the surface inclination and surface tension. For a given Weber number, emission of secondary droplet takes place at the earliest time for surfactant solution due to reduction of interfacial energy.</p>
17.	<p>Effect of Voltage Waveforms of HVDC Converter Transformer on Lifetime Characteristics B Singh, AJJ Thomas, CC Reddy - IEEE Transactions on Power Delivery, 2020</p> <p>Abstract: The converter transformers are reported to fail generally on the thyristor-valve side, where complex alternating voltage waveforms superimposed with dc voltages would occur. The effect of these waveforms on the failure and endurance of the valve side winding insulation of the transformers is not yet understood, which is investigated here. In this paper, the voltage waveforms occurring in a converter transformer are obtained through PSCAD/EMTDC for a typical double pole ± 500 kV, 1000 MW DC-link HVDC transmission system based on the CIGRE benchmark system. The waveforms are then amplified using a High Voltage amplifier for experimental breakdown investigations. Stepped-stress damage equalization method has been used for obtaining the lifetime characteristics from failure data. A comparison with life curve under pure sinusoidal and actual alternating voltages with superimposed dc and harmonic voltage has been made to</p>

	<p>understand why the converter transformers generally failed on the valve side. The results first time give fundamental reasons for the possible failure of the converter transformers and put forth important design considerations.</p>
18.	<p>Efficient chemical fixation of CO₂ from direct air under environment-friendly co-catalyst and solvent-free ambient conditions R Das, T Ezhil, AS Palakkal, D Muthukumar, RS Pillai, CM Nagaraja - Journal of Materials Chemistry A, 2021</p> <p>Abstract: The capture and conversion of CO₂ from direct air into value-added products under mild conditions represents a promising step towards environmental remediation and energy sustainability. Consequently, herein, we report the first example of a Mg(II)-based MOF exhibiting highly efficient fixation of CO₂ from direct air into value-added cyclic carbonates under eco-friendly co-catalyst and solvent-free mild conditions. The bifunctional MOF catalyst was rationally constructed by utilizing an eco-friendly Lewis acidic metal ion, Mg(II), and a nitrogen-rich tripodal linker, TATAB. The MOF possesses a high BET surface area of 2606.13 m² g⁻¹ and highly polar 1D channels decorated with a high density of CO₂-philic sites which promote a remarkably high CO₂ uptake of 50.2 wt% at 273 K with a high heat of adsorption value of 55.13 kJ mol⁻¹. The high CO₂-affinity combined with the presence of a high density of nucleophilic and Lewis acidic sites conferred efficient catalytic properties to the Mg-MOF for chemical fixation of CO₂ from direct air under environment-friendly mild conditions. The remarkable performance of the Mg-MOF for the fixation of CO₂ from direct air was further supported by in-depth theoretical calculations. Moreover, the computational studies provided an insight into the mechanistic details of the catalytic process in the absence of any co-catalyst and solvent. Overall, this work represents a rare demonstration of carbon capture and utilization (CCU) from direct air under eco-friendly mild conditions.</p> 
19.	<p>Enhanced overall water splitting under visible light of MoSSe WSSe heterojunction by lateral interfacial engineering X Yang, JPA Wörnå, J Wang, P Zhang, W Luo, R Ahuja - Journal of Catalysis, 2021</p> <p>Abstract: Photocatalytic splitting water is a promising method to obtain hydrogen energy. While design and synthesis of efficient and economical photocatalysts is one of the important contents. Janus MoSSe and WSSe monolayers are efficient and wide sunlight harvesting photocatalysts due to their intrinsic vertical electric fields. So how is the photocatalytic performance of lateral MoSSe WSSe heterojunctions, which possesses an intra-plane interface and intrinsic vertical electric field? In the present work, the structural property, electronic characteristic, optical property, and photocatalytic application of MoSSe WSSe lateral heterojunctions are systematically investigated. It is found that both zigzag and armchair configurations are semiconductors with suitable bandgaps of ~1.60 eV. Besides, they possess a type-II band alignment where electrons tend to accumulate at the coupling interface of MoSSe side and holes at WSSe side, giving rise to a paralleled electric field in heterojunctions, which can largely promote the separation of photo-generated carriers. More remarkably, these heterojunctions exhibit pronounced solar-spectrum absorption efficiency, proper valence, and conduction band positions by initializing the redox reactions of H₂O and high carrier mobility. Intriguingly, the zigzag MoSSe WSSe heterojunction has a better photocatalytic performance in an acidic environment, and the armchair MoSSe WSSe</p>

prefers to produce H_2 and O_2 in a neutral environment. These fascinating properties render the intra-plane MoSSe|WSSe heterojunctions as the wide solar harvesting photocatalysts in further overall water splitting.



[Evaluation of Properties of Glow Discharge Plasma Nitrided C-300 Maraging Steel](#)

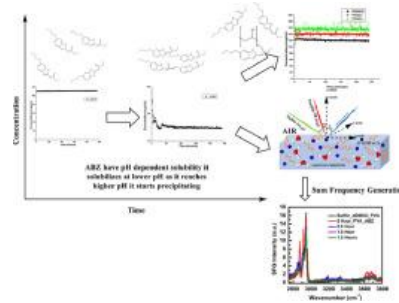
N Kumar, B Ganguli, S Sharma, B Roy, S Dixit - Transactions of the Indian Institute of Metals, 2021

20. **Abstract:** In this study, Glow Discharge Plasma Nitriding (GD_PN) of C-300 maraging steel is conducted at 425 °C to 500 °C for 4 h using H_2 and N_2 in a ratio of 4:1. The GD_PN treated surface is characterized by XRD and SEM and assessed for micro-hardness, tensile strength, corrosion as well as wear resistance. The micro-hardness measurements show an improvement in the hardness of the samples' surface by an approximate factor of 3.2. In the context of the case depth, it varies from 11.53 μm for 425 °C to 92.58 μm for 500 °C. The wear test results show improvement in wear resistance by a factor of 23.46 for treatment at 490 °C compared to the untreated sample. The tensile tests indicate that the ultimate tensile strength increases by a factor of 2.23 for treatment at 490 °C in comparison with the untreated sample. The XRD results depict that the plasma nitrided layer is incorporated with $\gamma'-Fe_4N$ as well as $\epsilon-Fe_{2-3}N$ phase. Finally, best corrosion resistance is observed for maraging steel sample treated at 490 °C.

[Explicating the molecular level drug-polymer interactions at the interface of supersaturated solution of the model drug: Albendazole](#)

P Joshi, P Mallepogu, H Kaur, R Singh, I Sodhi... KC Jena - European Journal of Pharmaceutical Sciences, 2021

21. **Abstract:** Supersaturation as a formulation principle relates to the aqueous solubility of poorly soluble drugs in solution. However, supersaturation state of drugs tends to crystallize because of its thermodynamic instability thereby compromising the solubility and biopharmaceutical performance of drugs. The present study aims to investigate the supersaturation potential of albendazole (ABZ) and its precipitation via nucleation and crystal growth. We hypothesized the use of polymers will avoid ABZ precipitation by interacting with drug molecules. The drug polymer interactions are characterized using conventional methods of Fourier transform infrared (FTIR), Nuclear magnetic resonance (NMR) and Polarized light microscopy (PLM). We have used a novel approach of sum frequency generation (SFG) vibrational spectroscopic in exploring the drug polymer interactions at air-water interface. Recently we have reported the SFG for rifaximin-polymer interactions (Singh et al., 2021). The supersaturation assay, saturation solubility studies and nucleation induction time analysis revealed polyvinyl alcohol (PVA) and polyvinyl pyrrolidone (PVP K30) as effective precipitation inhibitors thereby enhancing the ABZ equilibrium solubility and in vitro supersaturation maintenance of ABZ. Further, modification in the solid state of ABZ has confirmed the influence of polymers on its precipitation behaviour. We conclude that PVA and PVP K30 act as nucleation and crystal growth inhibitor, respectively for the precipitation inhibition of ABZ.

Graphical Abstract:**[Finite element modeling of ultrasonic assisted turning with external heating](#)****[J Airao, CK Nirala - Procedia CIRP, 2021](#)**

22. **Abstract:** Ultrasonic assisted turning (UAT) has shown significant advantages over conventional turning (CT) due to its intermittent cutting nature. There have been some issues related to the machining responses which have not been much explored. Most of the issues are driven by the cutting force which is a function of material properties. Present article gives finite element modeling (FEM) of UAT with external heating at different temperature assuming it alters the material properties particularly in terms of material softening. The objective is to analyze the effect of temperature, vibration amplitude, frequency and cutting speed on the machining responses using two different materials SS304 and low carbon (0.08%) steel. The parameters such as feed rate, tool rake angle and nose radius are kept constant. The shear angle, cutting force, and thrust force are determined as output responses. The FEM results show a significant effect of external heating in shear angle, cutting force and thrust force for both SS304 and low carbon steel. It is observed that as the temperature increases, there is an increment in shear angle and reduction in average cutting force and average thrust force. Moreover, a significant improvement in machining forces and shear angle was also noticed at a higher value of amplitude, cutting speed and frequency.

[Global presence of open-source research data management platform for libraries: the Dataverse project](#)**[V Jamwal, S Kaur - Library Hi Tech News, 2021](#)**

23. **Abstract:**
Purpose
This paper aims to provide statistical information on the worldwide spread of the open-source research data management application, the Dataverse Project, to librarians, data managers and information managers who are considering using the application at their own institution.
- Design/methodology/approach**
To produce a list of dataverse repositories, the official Dataverse website was evaluated, and JSON data were downloaded and parsed. Data standardisation was performed to assess the state of installations in various nations and continents across the world.
- Findings**
Globally, the Dataverse repositories have seen a rise in overall installations. The year 2020 alone saw a 23.21% rise. In a country-by-country comparison, the USA (13) has the most dataverse installations, while Europe (25) has the highest number of installations worldwide.
- Originality/value**
This research will be useful to librarians, data managers and information managers, among others, who want to learn more about Dataverse repositories throughout the world before deploying at their local level.

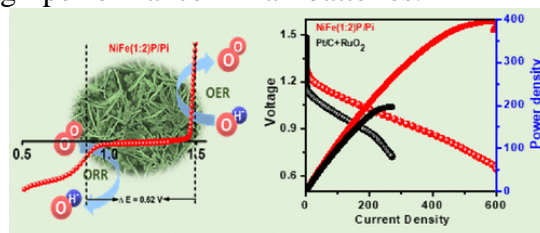
24.	<p>Head Matters: Explainable Human-centered Trait Prediction from Head Motion Dynamics S Madan, M Gahalawat, T Guha, R Subramanian - Proceedings of the 2021 International Conference on Multimodal Interaction, 2021</p> <p>Abstract: We demonstrate the utility of elementary head-motion units termed kinemes for behavioral analytics to predict personality and interview traits. Transforming head-motion patterns into a sequence of kinemes facilitates discovery of latent temporal signatures characterizing the targeted traits, thereby enabling both efficient and explainable trait prediction. Utilizing Kinemes and Facial Action Coding System (FACS) features to predict (a) OCEAN personality traits on the First Impressions Candidate Screening videos, and (b) Interview traits on the MIT dataset, we note that: (1) A Long-Short Term Memory (LSTM) network trained with kineme sequences performs better than or similar to a Convolutional Neural Network (CNN) trained with facial images; (2) Accurate predictions and explanations are achieved on combining FACS action units (AUs) with kinemes, and (3) Prediction performance is affected by the time-length over which head and facial movements are observed.</p>
25.	<p>Highly sensitive non-enzymatic electrochemical glucose sensor surpassing water oxidation interference N Thakur, D Mandal, TC Nagaiah - Journal of Materials Chemistry B, 2021</p> <p>Abstract: An electrochemical non-enzymatic sensor based on a NiVP/Pi material was developed for the selective and sensitive determination of glucose. The novel sensor showed a high sensitivity of $6.04 \text{ mA } \mu\text{M}^{-1} \text{ cm}^{-2}$ with a lowest detection limit of 3.7 nM in a wide detection range of 100 nM–10 mM. The proposed sensor exhibited a superior selectivity without any interference from the oxygen evolution reaction during glucose sensing. We also found that this glucose sensor showed negligible interference from various interferents, such as ascorbic acid, uric acid, dopamine and sodium chloride. Additionally, a novel flexible sensor was developed by coating the NiVP/Pi over Whatman filter paper, which exhibited two linear ranges of 100 nM to $1 \text{ } \mu\text{M}$ and $100 \text{ } \mu\text{M}$ to 10 mM with an ultra-sensitivity of $1.130 \text{ mA } \mu\text{M}^{-1} \text{ cm}^{-2}$ and $0.746 \text{ mA } \mu\text{M}^{-1} \text{ cm}^{-2}$, respectively, in 0.1 M NaOH. The proposed sensor was tested with human blood serum samples demonstrating its practical application. Our findings provide a new route by fine tuning the composition of nickel and vanadium that sheds new light on better understanding the processes. This NiVP/Pi-based sensor offers a new approach towards the electrochemical detection of glucose, enabling glucose monitoring in a convenient way.</p>
26.	<p>How well do the students understand the course contents? Assessing comprehension through course videos S Setia, SRS Iyengar, A Chhabra, AA Verma, N Dubey - Journal of Computers in Education, 2021</p> <p>Abstract: The popularity of MOOCs as an online education delivery alternative can be judged from the rapid increase in the number of MOOCs from the past few years. However, there are alarming concerns about the high drop-out ratios witnessed by the MOOCs. Several factors such as poor student engagement, poor lecture delivery in videos, low student–instructor interaction are known to be responsible for declining completion rates in MOOCs. Out of these, the current work focuses on poor student engagement. Many of the students tend to lose interest in the course since they are unable to follow course videos. Hence, one of the methods to quantify student engagement is to study the comprehension of course contents perceived by the students after watching the course videos. For this, we deploy a collaborative portal, named QWiki, as a part of a MOOC. QWiki is a combination of a QnA forum and a wiki portal that houses student-generated data. The student-generated data from QWiki helps evaluate the comprehension of course contents by the students. We analyze and put forth results for a MOOC based on Python programming.</p>

27.	<p>Hyperrealistic Image Inpainting with Hypergraphs G Wadhwa, A Dhall, S Murala... - Proceedings of the IEEE/CVF Winter Conference on Applications of Computer Vision, 2021</p> <p>Abstract: Image inpainting is a non-trivial task in computer vision due to multiple possibilities for filling the missing data, which may be dependent on the global information of the image. Most of the existing approaches use the attention mechanism to learn the global context of the image. This attention mechanism produces semantically plausible but blurry results because of incapability to capture the global context. In this paper, we introduce hypergraph convolution on spatial features to learn the complex relationship among the data. We introduce a trainable mechanism to connect nodes using hyperedges for hypergraph convolution. To the best of our knowledge, hypergraph convolution have never been used on spatial features for any image-to-image tasks in computer vision. Further, we introduce gated convolution in the discriminator to enforce local consistency in the predicted image. The experiments on Places2, CelebA-HQ, Paris Street View, and Facades datasets, show that our approach achieves state-of-the-art results.</p>
28.	<p>Implicit Visual Attention Feedback System for Wikipedia Users N Dubey, AA Verma, SRS Iyengar, S Setia - 17th International Symposium on Open Collaboration, 2021</p> <p>Abstract: The complex collaborative structure of Wikipedia has attracted researchers from various domains, such as social networks, human-computer interaction, and collective intelligence. Yet, a few focus on the readers' perception of Wikipedia. Readers make up the majority of Wikipedia users (editors/readers), and being on the consumption side, readers play a crucial role in its sustenance. The attention patterns of users while reading an article can reveal users' interest distribution as well as content quality of the article. In this paper, we present an Attention Feedback (AF) approach for Wikipedia readers. The fundamental idea of the proposed approach comprises the implicit capture of gaze-based feedback of Wikipedia readers using a commodity gaze tracker. The developed AF mechanism aims at overcoming the main limitation of the currently used "pageview" and "survey" based feedback approaches, i.e., data inaccuracy. Moreover, the incorporation of a single-camera image processing-based gaze tracker makes the overall system cost-efficient and portable. The proposed approach can be extended to enable the research community to analyze various online portals as well as offline documents from the readers' perspective.</p>
29.	<p>Influence of contact geometry on NTD sensor performance V Vatsa, A Reza, A Mazumdar, V Nanal, RG Pillay... - IEEE 14th Workshop on Low Temperature Electronics, 2021</p> <p>Abstract: A cryogenic bolometer with Neutron Transmutation Doped Ge as mK thermometer is being developed to study neutrinoless double beta decay (NDBD) in ^{124}Sn. The performance and sensitivity of the sensor strongly depends on the irradiation as well as fabrication (etching, annealing, contact deposition) process. The role of contact fabrication on the sensor performance is presented here. The performance of NTD Ge sensors with wrap-around contact and face-type contacts is compared at $T < 100$ mK. It is observed that NTD Ge sensors with face-type contacts show Mott behaviour upto lower temperature ~ 35 mK as compared to that for sensors with wrap-around contacts. Further, detailed noise measurements on several indigenously developed NTD Ge sensors have been carried out in temperature range of 20-70 mK to understand its impact on bolometer resolution and have been described in following section.</p>

30.	<p>Local electrocatalytic activity of PtRu supported on nitrogen-doped carbon nanotubes towards methanol oxidation by scanning electrochemical microscopy D Gupta, S Chakraborty, RG Amorim, R Ahuja, TC Nagaiah - Journal of Materials Chemistry A, 2021</p> <p>Abstract: Nitrogen-doped carbon nanotubes (NCNTs) were synthesized by treating HNO₃-oxidized carbon nanotubes (CNTs) in an NH₃ flow at different temperatures. PtRu nanoparticles were decorated over NCNTs. The PtRu catalysts were prepared by an impregnation–reduction method from metal chloride precursors with a total metal loading of about 10 wt%. The electrocatalytic activity with respect to methanol oxidation was studied using electrochemical and scanning electrochemical microscopy (SECM) measurements. Transmission electron microscopy revealed the spherical shape and narrow particle size distribution of the PtRu particles over NCNTs with average particle sizes of ~3–5 nm. A detailed X-ray photoelectron spectroscopy study was performed to quantitatively identify different nitrogen functional groups and to evaluate their role in the observed enhanced catalytic activity towards methanol oxidation. The determination of the local electrocatalytic activity of the proposed catalyst towards methanol oxidation and simultaneous evaluation of the intermediates produced during methanol oxidation were achieved using SECM. Density functional theory studies were performed to understand the adsorption sites of methanol and intermediates on different reactive sites and to investigate possible reaction mechanisms.</p>
31.	<p>Micro-machining: An overview (Part II) VK Jain, DS Patel, J Ramkumar, B Bhattacharyya, S Sankar, AD Jayal - Journal of Micromanufacturing, 2021</p> <p>Abstract: This article on ‘Micro-machining: An Overview (Part II)’ is in continuation to ‘Micro-machining: An Overview (Part I)’ published in this journal (Journal of Micromanufacturing). It consists of four parts, namely, electrochemical micro-texturing, electrochemical spark micro-machining, molecular dynamics simulation and sustainability issues of micro-machining processes. Electrochemical micro-texturing (ECMTex) deals with various techniques developed for micro-texturing on different types of workpiece-surfaces, namely, flat, curved and free-form surfaces. Here, basically two categories of techniques have been reviewed, namely, with mask and without mask. It also deals with ‘single point tool micro-texturing’ which turns out to be a single-step technique requiring minimum time, but the accuracy and repeatability obtained after micro-texturing need to be critically analysed. For mass production, one needs to go for sinking kind of ECMTex processes.</p> <p>Electrochemical spark micro-machining (ECSMM) is an interesting hybrid (ECM+EDM) process which can be applied for electrically conducting as well as electrically non-conducting materials. However, the work reported in this article deals only with the electrically non-conducting materials for which this process was initially developed. This process has a lot of potential for theoretical work to be done. In this article, two theories of sparking/discharging have been briefly mentioned: single bubble discharging/sparking and single surface discharging. It also discusses its applications for different types of electrically non-conducting materials.</p> <p>Molecular dynamics simulation (MDS) of micro-/nano-machining processes is very important, but it is very cumbersome to understand at atomic/molecular scale. In these processes, the material behaviour at micro-/nano-level machining is completely different as compared to bulk-machining (macro-machining) processes. Hence, some fundamentals of MDS have been discussed. It just gives the idea of available techniques, softwares and models for different types of processes. However, there is the need of further research work to be done for clearly understanding the MDS of micro-/nano-machining.</p> <p>In the end, the sustainability of micro-machining issues have been discussed, mainly based on the energy consumption per unit mass of production. It is concluded that the advanced micro-</p>

	<p>manufacturing processes are highly energy-intensive processes, and they need further studies to be done for making them more suitable from sustainability point of view.</p> <p>At the end of each section, some potential areas of research for enhancing the accuracy and repeatability, and minimising the production time of each process have been discussed.</p>
32.	<p>Multi-frame Recurrent Adversarial Network for Moving Object Segmentation PW Patil, A Dudhane, S Murala - Proceedings of the IEEE/CVF Winter Conference on Applications of Computer Vision, 2021</p> <p>Abstract: Moving object segmentation (MOS) in different practical scenarios like weather degraded, dynamic background, etc. videos is a challenging and high demanding task for various computer vision applications. Existing supervised approaches achieve remarkable performance with complicated training or extensive fine-tuning or inappropriate training-testing data distribution. Also, the generalized effect of existing works with completely unseen data is difficult to identify. In this work, the recurrent feature sharing based generative adversarial network is proposed with unseen video analysis. The proposed network comprises of dilated convolution to extract the spatial features at multiple scales. Along with the temporally sampled multiple frames, previous frame output is considered as input to the network. As the motion is very minute between the two consecutive frames, the previous frame decoder features are shared with encoder features recurrently for current frame foreground segmentation. This recurrent feature sharing of different layers helps the encoder network to learn the hierarchical interactions between the motion and appearance based features. Also, the learning of the proposed network is concentrated in different ways, like disjoint and global training-testing for MOS. An extensive experimental analysis of the proposed network is carried out on two benchmark video datasets with seen and unseen MOS video. Qualitative and quantitative experimental study shows that the proposed network outperforms the existing methods.</p>
33.	<p>MXene binder stabilizes pseudocapacitance of conducting polymers M Boota, E Jung, R Ahuja, T Hussain - Journal of Materials Chemistry A, 2021</p> <p>Abstract: Conducting polymers (CPs) are by far the most studied organic materials for supercapacitors. Yet, their structural instability stemming from volumetric expansion/contraction during charge/discharge results in capacitance loss after moderate cycling that limits their applications. Here, we show that the remarkable cycling stability, capacitance, and rate performance can be achieved by replacing conventional electrode additives (carbon black or insulating polymer binder) with titanium carbide ($\text{Ti}_3\text{C}_2\text{T}_x$) MXene. Using polyaniline (PANI) as a model system, an addition of only 15 wt% of $\text{Ti}_3\text{C}_2\text{T}_x$ MXene binder delivered remarkable capacitance retention of 96% after 10 000 cycles at 50 mV s^{-1} and high-rate capability with a capacitance of 434 F g^{-1}. Using density functional theory (DFT) calculations, we show that, unlike insulating polymer binders, surface groups of MXene bond to PANI with a significantly high binding energy (up to -2.11 eV) via a charge transfer mechanism. This is one of the key mechanisms to achieve a high electrochemical performance of the CP-based electrodes when MXene is used as a binder. We expect that a similar approach can be used for stabilizing other organic electrode materials.</p>
34.	<p>Nickel Iron Phosphide/Phosphate as an Oxygen Bifunctional Electrocatalyst for High-Power-Density Rechargeable Zn–Air Batteries N Thakur, M Kumar, D Mandal, TC Nagaiah - ACS Applied Materials & Interfaces, 2021</p> <p>Abstract: The evolution of an effective oxygen electrocatalyst is of great importance for the widespread application of Zn–air batteries but remains an immense challenge. Thus, an efficient catalyst toward the oxygen evolution reaction and oxygen reduction reaction (OER and ORR) is highly essential for high-performance Zn–air batteries. Here, we have reported bifunctional nickel iron phosphide/phosphate (NiFeP/Pi) catalysts with various Ni/Fe ratios toward oxygen</p>

electrocatalysis in alkaline media. These catalysts are highly active toward OER and ORR, wherein NiFe(1:2)P/Pi exhibits a low OER overpotential of 0.21 V at 10 mA cm⁻² and a high ORR onset potential (0.98 V vs RHE) with the lowest potential difference ($\Delta E = E_{10} - E_{1/2}$) of 0.62 V, which surpasses that of the benchmark Pt/C and RuO₂ catalyst as well as those of most previously reported bifunctional catalysts. Furthermore, the NiFe(1:2)P/Pi-based Zn–air battery demonstrates a very high power density of 395 mW cm⁻² and outstanding discharge capacity of 900 mAh g⁻¹ @ 10 mA cm⁻² along with steady cyclability, maintaining 98% of the round trip efficiency over 300 cycles. These results are helpful for a good understanding of the composition–activity relation with a certain band gap toward high-performance Zn–air batteries.



[On duality gap as a measure for monitoring gan training](#)

S Sidheekh, A Aimen, V Madan, NC Krishnan - International Joint Conference on Neural Networks, 2021

35.

Abstract: Generative adversarial networks (GANs) are among the most popular deep learning models for learning complex data distributions. However, training a GAN is known to be a challenging task. This is often attributed to the lack of correlation between the training progress and the trajectory of the generator and discriminator losses and the need for the GAN's subjective evaluation. A recently proposed measure inspired by game theory - the duality gap, aims to bridge this gap. However, as we demonstrate, the duality gap's capability remains constrained due to limitations posed by its estimation process. This paper presents a theoretical understanding of this limitation and proposes a more dependable estimation process for the duality gap. At the crux of our approach is the idea that local perturbations can help agents in a zero-sum game escape non-Nash saddle points efficiently. Through exhaustive experimentation across GAN models and datasets, we establish the efficacy of our approach in capturing the GAN training progress with minimal increase to the computational complexity. Further, we show that our estimate, with its ability to identify model convergence/divergence, is a potential performance measure that can be used to tune the hyperparameters of a GAN.

[PACE: Posthoc Architecture-Agnostic Concept Extractor for Explaining CNNs](#)

V Kamakshi, U Gupta, NC Krishnan – IEEE International Joint Conference on Neural Networks , 2021

36.

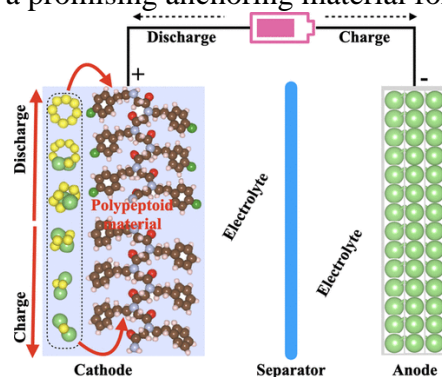
Abstract: Deep CNNs, though have achieved the state of the art performance in image classification tasks, remain a black-box to a human using them. There is a growing interest in explaining the working of these deep models to improve their trustworthiness. In this paper, we introduce a Posthoc Architecture-agnostic Concept Extractor (PACE) that automatically extracts smaller sub-regions of the image called concepts relevant to the black-box prediction. PACE tightly integrates the faithfulness of the explanatory framework to the black-box model. To the best of our knowledge, this is the first work that extracts class-specific discriminative concepts in a posthoc manner automatically. The PACE framework is used to generate explanations for two different CNN architectures trained for classifying the AWA2 and Imagenet- Birds datasets. Extensive human subject experiments are conducted to validate the human interpretability and consistency of the explanations extracted by PACE. The results from these experiments suggest that over 72% of the concepts extracted by PACE are human interpretable.

[Polypeptoid Material as an Anchoring Material for Li-S Batteries](#)

D Singh, R Ahuja - ACS Applied Energy Materials, 2021

37.

Abstract: Nowadays, lithium-sulfur (Li-S) batteries have attracted considerable attention as a potential candidate for next-generation rechargeable batteries due to their high theoretical specific energy and environmental friendliness. One of the main problems with Li-S batteries is that the lithium polysulfides (LiPSs) easily decompose in the electrolyte which is known as the shuttle effect. Recently, the polypeptoid nanosheet crystal structure has been experimentally synthesized which is very useful for tremendous advances in soft material imaging as well as enabling to design biomimetic nanomaterials. Due to the very interesting properties of the polypeptoid material, we have investigated the electronic structure and charge-transfer mechanism for the lithium-sulfur batteries for the cathode material. The calculated adsorption energies of LiPSs on the surface of the polypeptoid material are in the range of -4.41 to -4.64 and -0.91 eV for the sulfur clusters. Also, the adsorption energies between the interaction of LiPSs and electrolytes (DME and DOL) are 0.75 – 0.89 eV. It means that the polypeptoid material could suppress the shuttle effect of LiPSs and significantly enhance the cycling performance of Li-S batteries. From these investigated results, the polypeptoid material will be a promising anchoring material for Li-S batteries.



[Pressure-induced order-disorder transitions in \$\beta\$ - \$\text{In}_2\text{S}_3\$: an experimental and theoretical study of structural and vibrational properties](#)

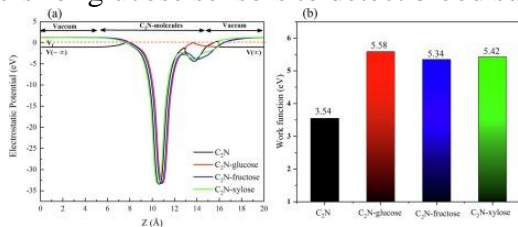
S Gallego-Parra, Ó Gomis, R Vilaplana... R Ahuja... - ... Chemistry Chemical Physics, 2021

38.

Abstract: This joint experimental and theoretical study of the structural and vibrational properties of β - In_2S_3 upon compression shows that this tetragonal defect spinel undergoes two reversible pressure-induced order-disorder transitions up to 20 GPa. We propose that the first high-pressure phase above 5.0 GPa has the cubic defect spinel structure of α - In_2S_3 and the second high-pressure phase (ϕ - In_2S_3) above 10.5 GPa has a defect α - NaFeO_2 -type ($R\bar{3}m$) structure. This phase, related to the NaCl structure, has not been previously observed in spinels under compression and is related to both the tetradymite structure of topological insulators and to the defect LiTiO_2 phase observed at high pressure in other thiospinels. Structural characterization of the three phases shows that α - In_2S_3 is softer than β - In_2S_3 while ϕ - In_2S_3 is harder than β - In_2S_3 . Vibrational characterization of the three phases is also provided, and their Raman-active modes are tentatively assigned. Our work shows that the metastable α phase of In_2S_3 can be accessed not only by high temperature or varying composition, but also by high pressure. On top of that, the pressure-induced β - α - ϕ sequence of phase transitions evidences that β - In_2S_3 , a $\text{B}^{\text{III}}_2\text{X}^{\text{V}}_3$ compound with an intriguing structure typical of $\text{A}^{\text{II}}\text{B}^{\text{III}}_2\text{X}^{\text{VI}}_4$ compounds (intermediate between thiospinels and ordered-vacancy compounds) undergoes: (i) a first phase transition at ambient pressure to a disordered spinel-type structure (α - In_2S_3), isostructural with those found at high pressure and high temperature in other $\text{B}^{\text{III}}_2\text{X}^{\text{V}}_3$ compounds; and (ii) a second phase transition to the defect α - NaFeO_2 -type structure (ϕ - In_2S_3), a distorted NaCl-type structure that is related to the defect NaCl phase found at high pressure in $\text{A}^{\text{II}}\text{B}^{\text{III}}_2\text{X}^{\text{VI}}_4$ ordered-vacancy compounds and to the defect LiTiO_2 -type phase found at high pressure in $\text{A}^{\text{II}}\text{B}^{\text{III}}_2\text{X}^{\text{VI}}_4$ thiospinels. This result shows that In_2S_3 (with its intrinsic vacancies)

	has a similar pressure behaviour to thiospinels and ordered-vacancy compounds of the $A^{II}B^{III}_2X^{VI}_4$ family, making $\beta\text{-In}_2\text{S}_3$ the union link between such families of compounds and showing that group-13 thiospinels have more in common with ordered-vacancy compounds than with oxospinel and thiospinels with transition metals.
39.	<p>Qualifying carbon nanotube reinforced polyurethane foam as helmet inner liner through in-situ, static and low velocity impact testing J Bhinder, SK Verma, PK Agnihotri - Materials Science and Engineering: B, 2021</p> <p>Abstract: Helmet inner liner (HIL) is a critical component of helmets which ensures safety and comfort of the wearer. Efforts are made in this work to qualify polyurethane (PU) foams for HIL application. Processing temperature and weight fraction of carbon nanotubes (CNTs) nanofillers is varied to optimize the microstructure and hence average properties of PU foams. Experimental results show that PU foam processed at -5°C and reinforced with 1.6 wt% of oxidized CNTs shows 40% higher specific elastic modulus and 11% better recovery under compression testing, absorbs 97% more energy per unit volume in comparison to EPS under low velocity impact in drop weight tests. The 34% higher thermal conductivity than EPS implies that it will provide better comfort by efficiently dissipating the heat generated in helmet. The superior combination of properties makes CNT reinforced PU foams a better alternative as HIL in comparison to currently used EPS foam.</p>
40.	<p>Semiconducting phase of hafnium dioxide under high pressure: a theoretical studied by quasi-particle GW calculations T Bovornratanaraks, R Ahuja... - Materials Research Express, 2021</p> <p>Abstract: The phase stability of the hafnium dioxide compounds HfO_2, a novel material with a wide range of application due to its versatility and biocompatibility, is predicted to be achievable by using evolutionary technique, based on first-principles calculations. Herein, the candidate structure of HfO_2 is revealed to adopt a tetragonal structure under high-pressure phase with $P4/nmm$ space group. This evidently confirms the stability of the HfO_2 structures, since the decomposition into the component elements under pressure does not occur until the pressure is at least 200 GPa. Moreover, phonon calculations can confirm that the $P4/nmm$ structure is dynamically stable. The $P4/nmm$ structure is mainly attributed to the semiconducting property within using the Perdew–Burke–Ernzerhof, the modified Becke–Johnson exchange potential in combination with the generalized gradient approximations, and the quasi-particle GW approximation, respectively. Our calculation manifests that the $P4/nmm$ structure is likely to be metal above 200 GPa, arising particularly from GW approximation. The remarkable results of this work provide more understanding of the high-pressure structure for designing metal-oxide-based semiconducting materials.</p>
41.	<p>Semipaired Domination in Some Subclasses of Chordal Graphs V Tripathi, A Pandey, V Tripathi - Discrete Mathematics & Theoretical Computer Science, 2021</p> <p>Abstract: A dominating set D of a graph G without isolated vertices is called semipaired dominating set if D can be partitioned into 2-element subsets such that the vertices in each set are at distance at most 2. The semipaired domination number, denoted by $\gamma_{pr2}(G)$ is the minimum cardinality of a semipaired dominating set of G. Given a graph G with no isolated vertices, the \textsc{Minimum Semipaired Domination} problem is to find a semipaired dominating set of G of cardinality $\gamma_{pr2}(G)$. The decision version of the \textsc{Minimum Semipaired Domination} problem is already known to be NP-complete for chordal graphs, an important graph class. In this paper, we show that the decision version of the \textsc{Minimum Semipaired Domination} problem remains NP-complete for split graphs, a subclass of chordal graphs. On the positive side, we propose a linear-time algorithm to compute a minimum cardinality semipaired dominating set of block graphs. In addition, we prove that the \textsc{Minimum Semipaired Domination} problem is APX-complete for graphs with maximum degree 3.</p>

42.	<p>Shadows of black hole surrounded by anisotropic fluid in Rastall theory R Kumar, BP Singh, MS Ali, SG Ghosh - Physics of the Dark Universe, 2021</p> <p>Abstract: Due to the gravitational lensing effect, a black hole casts a shadow larger than its horizon over a bright background, and the shape and size can be calculated. The Event Horizon Telescope collaboration has produced the first direct image (shadow) of the black hole and it is in accordance with the shadow of a Kerr black hole of general relativity. However deviations from the Kerr black hole arising from modified theories of gravity are not ruled out and they are important as they offer an arena to test these theories through astrophysical observation. This stimulates us to investigate rotating black holes surrounded by anisotropic fluid in Rastall theory namely a rotating Rastall black hole, which are characterized by mass M, spin a, field structure parameter N_s and the Rastall parameter ψ. It encompasses, as special cases, Kerr ($N_s \rightarrow 0$) and Kerr–Newman ($s=0$ and $N_s = -Q^2$) black holes. The rotating Rastall black hole is characterized by an additional cosmological-like horizon apart from Cauchy and event horizons. We derive an analytical formula for the shadow of a rotating Rastall black hole and go on to visualize the shadow of black holes for various values of the parameters for an observer at a given coordinates (r_0, θ_0) in the domain $[r_+, r_q]$.</p>
43.	<p>Situational Anomaly Detection in Multimedia Data under Concept Drift P Kumari - Proceedings of the 29th ACM International Conference on Multimedia, 2021</p> <p>Abstract: Anomaly detection has been a very challenging and active area of research for decades, particularly for video surveillance. However, most of the works detect predefined anomaly classes using static models. These frameworks have limited applicability for real-life surveillance where the data have concept drift. Under concept drift, the distribution of both normal and anomaly classes changes over time. An event may change its class from anomaly to normal or vice-versa. The non-adaptive frameworks do not handle this drift. Additionally, the focus has been on detecting local anomalies, such as a region of an image. In contrast, in CCTV-based monitoring, flagging unseen anomalous situations can be of greater interest. Utilizing multiple sensory information for anomaly detection has also received less attention. This extended abstract discusses these gaps and possible solutions.</p>
44.	<p>Structure-induced broadband tunable resonances in soft material based dielectric metasurfaces M Khokhar, RV Nair - Journal of Applied Physics, 2021</p> <p>Abstract: The dielectric metasurfaces using soft materials have generated opportunities in metamaterials by manipulating light interaction at a sub-wavelength scale. Here, we study the low-index dielectric metasurface consisting of a monolayer of dielectric micro-spheres in the visible region. The metasurface exhibits optical resonances, which appear as dips in the reflectivity spectra measured using the state-of-the-art micro-reflectivity facility. The origin of resonances is due to the diffraction of light on the corrugated surface, which appears as a grating mode or due to the light trapped within the micro-spheres termed as the leaky mode. The tunability of resonant modes is discussed as a function of the lattice constant and the effective refractive index of the metasurface. The experimental results are validated using the finite-difference time-domain simulations and theoretical calculations. The impact of the substrate refractive index is studied which shows higher refractive index contrast between the sample and the substrate, more light is confined within the metasurface. The proposed soft material-based metasurfaces can be used as a mask for making more complex photonic structures, generating structural coloration, and material base for rapid sensing.</p>
45.	<p>The Gordian complex of theta-curves S Joshi, M Prabhakar - Journal of Knot Theory and Its Ramifications, 2021</p> <p>Abstract: In this paper, we study the Gordian metric on the set of all theta-curves and give a lower bound of it. We define the Gordian complex of theta-curves, which is a simplicial complex whose vertices consist of all theta-curves in the 3-dimensional Euclidean space R^3. We show that for any</p>

	<p>given theta-curve Θ, there exists an infinite family of theta-curves containing Θ such that the Gordian distance between any two distinct members of this family is equal to one.</p>										
46.	<p>The Size-Dependent Catalytic Performances of Supported Metal Nanoparticles and Single Atoms for the Upgrading Biomass-Derived 5-Hydroxymethylfurfural , Furfural, and Levulinic acid R Srivastava, A Shivhare, A Kumar – ChemCatChem, 2021</p> <p>Abstract: The success of integrated biorefinery relies on developing robust and economical catalytic processes to produce liquid fuels and value-added chemicals from the waste lignocellulose biomass. Platform chemicals obtained from biomass are multifunctional molecules, and their upgrading via various catalytic processes requires active and selective catalysts. Supported transition metal nanoparticles have been used extensively to catalyze the upgrading of biomass-derived platform chemicals. Recent literature studies have focused on understanding the size-dependent catalytic performances of supported transition metal nanoparticles and single atoms in biomass-related chemical transformations. The catalytic behavior of transition metals depends on their size-dependent geometric and electronic structures, and by controlling the size, the catalytic behavior can be optimized. Herein, we have reviewed the synthesis methodologies and characterization techniques of supported metal nanoparticles of different sizes and supported single atoms and have summarized several literature examples employing these catalysts to upgrade biomass-derived platform chemicals such as; 5-hydroxymethylfurfural, furfural, and levulinic acid, into liquid fuels and value-added chemicals.</p>										
47.	<p>Two-Dimensional Nitrogenated Holey Graphene (C₂N) Monolayer Based Glucose Sensor for Diabetes Mellitus P Panigrahi, M Sajjad, D Singh, T Hussain... R Ahuja... - Applied Surface Science, 2021</p> <p>Abstract: Real-time monitoring of sugar molecules is crucial for diagnosis, controlling, and preventing diabetes. Here, we have proposed the potential of porous C₂N monolayer-based glucose sensor to detect the sugar molecules (glucose, fructose, and xylose) by employing the van der Waals interactions corrected first-principles density functional theory and non-equilibrium Green's function methods. The binding energy turns out to be -0.93 (-1.31) eV for glucose, -0.84 (-1.23) eV for fructose, and -0.81 (-1.30) eV for xylose in gas phase (aqueous medium). The Bader charge analysis reveals that the C₂N monolayer donates charge to the sugar molecules. The dimensionless electron localization function highlights that glucose, fructose, and xylose bind through physisorption. The adsorption of sugar molecules on the C₂N monolayer increases the workfunction compared to 3.54 eV (pristine C₂N) with about 2.00 eV, indicating a suppressed probability of electron mobility. The electronic transport properties of C₂N based device reveals distinct characteristics and zero-bias transmissions. The distinctive properties of the C₂N monolayer can be indexed as promising identifiers for glucose sensors to detect blood sugar.</p>  <p>Figure (a) shows the Electronic Potential (eV) versus Z (Å) for C₂N monolayer and its interaction with glucose, fructose, and xylose. The potential curves show a significant dip at the adsorption site. Figure (b) is a bar chart showing the Work function (eV) for C₂N and its complexes with glucose, fructose, and xylose. The work function increases from 3.54 eV for pristine C₂N to 5.58 eV for C₂N-glucose, 5.34 eV for C₂N-fructose, and 5.43 eV for C₂N-xylose.</p> <table border="1"> <thead> <tr> <th>System</th> <th>Work function (eV)</th> </tr> </thead> <tbody> <tr> <td>C₂N</td> <td>3.54</td> </tr> <tr> <td>C₂N-glucose</td> <td>5.58</td> </tr> <tr> <td>C₂N-fructose</td> <td>5.34</td> </tr> <tr> <td>C₂N-xylose</td> <td>5.43</td> </tr> </tbody> </table>	System	Work function (eV)	C ₂ N	3.54	C ₂ N-glucose	5.58	C ₂ N-fructose	5.34	C ₂ N-xylose	5.43
System	Work function (eV)										
C ₂ N	3.54										
C ₂ N-glucose	5.58										
C ₂ N-fructose	5.34										
C ₂ N-xylose	5.43										
48.	<p>UAV Deployment for Throughput Maximization in a UAV-Assisted Cellular Communications N Gupta, S Agarwal, D Mishra - IEEE 32nd Annual International Symposium on Personal, Indoor and Mobile Radio Communications, 2021</p> <p>Abstract: Unmanned Aerial Vehicle (UAV) deployment as an aerial base station in fifth-generation (5G) communication system has emerged as a promising technology to provide seamless communication in a geographical region. The UAV's high mobility potential offers additional degrees of freedom for effective deployment. Therefore, the three-dimensional (3D)</p>										

	<p>deployment of UAV is one of the key challenges in UAV-assisted communication systems. In this paper, we address the problem of UAV deployment in 3D space to provide on-demand coverage to the ground users to maximize the sum rate. We consider realistic UAV-ground channel model derived from extensive experiments. The problem formulated is non-convex. To obtain the optimal location, we approximate the rate expression to identify the concave regions and propose a low-complexity solution by applying alternating optimization. Through simulation results, we provide valuable insights into the low-complexity solution.</p>
49.	<p><u>UW-GAN: Single Image Depth Estimation and Image Enhancement for Underwater Images</u> P Hambarde, S Murala, A Dhall - <i>IEEE Transactions on Instrumentation and Measurement</i>, 2021</p> <p>Abstract: Due to the unavailability of large scale underwater depth image datasets and ill-posed problems, underwater single image depth prediction is a challenging task. An unambiguous depth prediction for single underwater image is an essential part of applications like underwater robotics, marine engineering, etc. This paper presents an end-to-end Underwater Generative Adversarial Network (UW-GAN) for depth estimation from an underwater single image. Initially, a coarse-level depth map is estimated using the Underwater Coarse-level Generative Network (UWC-Net). Then, a fine-level depth map is computed using the Underwater Fine-level Network (UWF-Net) which takes input as the concatenation of the estimated coarse-level depth map and the input image. The proposed UWF-Net comprises of spatial and channel-wise squeeze and excitation block for fine-level depth estimation. Also, we propose a synthetic underwater image generation approach for large scale database. The proposed network is tested on real-world and synthetic underwater datasets for its performance analysis. We also perform a complete evaluation of the proposed UW-GAN on underwater images having different color domination, contrast, and lighting conditions. Presented UW-GAN framework is also investigated for underwater single image enhancement. Extensive result analysis proves the superiority of proposed UW-GAN over the state-of-the-art hand-crafted, and learning based approaches for underwater single image depth estimation and enhancement.</p>

Disclaimer: This publication digest may not contain all the papers published. Library has compiled the publication data as per the alerts received from Scopus and Google Scholar for the affiliation “Indian Institute of Technology Ropar” for the month of October 2021. The author(s) are requested to share their missing paper(s) details if any, for the inclusion in the next publication digest.